Iranian Journal of Microbiology

Volume 17 Number 5 (October 2025) 826-834
DOI: http://doi.org/10.18502/ijm.v17i5.19891

ORIGINAL ARTICLE

SARS-CoV-2 mRNA vaccine candidate encoding RBD chimera of Delta and Omicron variants: immunogenic potential and validation

Shahla Shahsavandi[1*], Sina Soleimani[1], Majid Tebyanian[1], Amir Ali Hariri[2], Ashraf Mohammadi[1], Abbas Zare Mirakabadi[1], Mojtaba Noofeli[1], Zarrin Sharifnia[2], Mohammad Mahdi Ranjbar[1]

[1]Razi Vaccine and Serum Research Institute, Agricultural Research Education and Extension Organization, Karaj, Iran
[2]Biotechnology Department, Behyaar Sanaat Sepahan Company, Isfahan, Iran

Received: March 2025**, Accepted:** September 2025

ABSTRACT

Background and Objectives: The emergence of severe acute respiratory syndrome coronavirus 2 (SARS-CoV-2) variants has presented a challenging issue for global health in the 21st century. Frequent mutations in viral genomes have diminished the effectiveness of current vaccines against new variants. Messenger RNA (mRNA) vaccine is a promising platform for eliciting a robust T cell immune response.

Materials and Methods: We evaluated the uptake of mRNA-LNPs into human monocyte-derived dendritic cells by measuring the intensity of enhanced eGFP expression in the transfected cells. Next, we assessed the effect of mRNA-LNPs on immune response induction in mice following a prime-boost immunization strategy, along with analyzing cytokine release. The safety of the vaccine candidate was examined through pyrogenicity and toxicity assays.

Results: Upon intramuscular injection of mice, potent antibodies specific to viral S protein, robust Th1-biased cell-mediated immunity, and enhanced IFN-γ expression were induced. These observations indicate that mRNA-LNP was taken up and that it migrated to the lymph nodes. Furthermore, the vaccine candidate did not cause inflammation or local reactions after injection, as confirmed by biochemical, hematological, and histopathological examinations.

Conclusion: Because of its ability to target immune cells, the mRNA vaccine candidate can potentially improve immune responses against circulating or emerging variants.

Keywords: SARS-CoV-2; mRNA vaccine; Receptor binding domain; Immunity

INTRODUCTION

The spread of severe acute respiratory syndrome coronavirus 2 (SARS-CoV-2) has led to loss of life and economic hardship during the 2019 COVID-19 pandemic (1). Since the outbreak of the pandemic, various vaccine development platforms have been established against SARS-CoV-2, including inactivated whole virus particle, ribonucleic acid, vectored, and protein subunit vaccines. However, only some of them have been approved for widespread use (2, 3). The most recent platform to evolve for introducing foreign antigens in vivo to induce immune responses is mRNA vaccines. While the concept of using mRNA in pharmacology began in 1989, significant progress has been made in developing messenger RNA (mRNA)-based vaccines during the COVID-19 pandemic (4).

*Corresponding author: Shahla Shahsavandi, Ph.D, Razi Vaccine and Serum Research Institute, Agricultural Research Education and Extension Organization, Karaj, Iran. Tel: +98-2634570038-46 Fax: +98-2634552194 Email: s.shahsavandi@rvsri.ac.ir

In vitro transcribed (IVT) mRNA carries the instructions for making specific proteins by encoding relevant antigens. This mRNA provides cells with a blueprint, which is then used by ribosomes to produce the desired proteins. Normally, IVT mRNA consists of an open reading frame, a 5′ cap, a 3′ poly (A) tail produced from a linear DNA template using an RNA polymerase, and flanking untranslated regions (UTRs) (5). The stability and ability of mRNA to be translated are key factors in the effectiveness of vaccines. The 5' and 3' UTRs play a strong role in determining these properties. Adding a cap and an optimal length of poly (A) tail are important for optimizing mRNA translation and stability, as well as increasing protein production. Increasing the G:C percentage and replacing rare codons with frequently used synonymous codons are other forms of sequence optimization that lead to increased steady-state mRNA levels and protein expression (6, 7). The role of these issues has already been discussed extensively. Moving beyond the role of these regulatory elements, the great challenge remains the effective delivery of mRNA into the cell. Induction of immunity is contingent upon the delivery of mRNA into the antigen-presenting cells (APCs). Therefore, IVT-mRNA needs a delivery system to facilitate cytosolic localization and enable efficient protein production. Because mRNA is easily broken down by ribonucleases, it can be degraded before it even reaches the target site. To solve this issue, various delivery systems have been developed. Encapsulating mRNA into lipid-based carriers enables quick uptake and expression of the molecule within the cytoplasm (8, 9).

The design technique of mRNA vaccines requires crucial mRNA modifications to optimize target protein expression and appropriate carrier formulations to ensure efficient cellular uptake. Following intramuscular injection, the cells process the delivered mRNA and express the target antigen via recruitment of immune cells. The FDA-approved SARS-CoV-2 mRNA vaccines are lipid nanoparticle (LNP)-based vaccines. Administration of mRNA-LNPs induces local infiltration of immune cells to the site of injection. Following an efficient internalization of mRNA-LNPs, monocytes and dendritic cells (DCs) translate the mRNA and upregulate cytokine production. LNPs offer many advantages, such as enhancing pharmacokinetic efficacy, increasing stability, and providing adjuvant properties for mRNA vaccines (10, 11). LNP-based mRNA vaccines contain an ionizable cationic lipid, cholesterol, a phospholipid, and a PEGylated lipid (12). In our previous studies, we designed the receptor binding domain (RBD)-dimer mRNA of Delta and Omicron variants construct, synthesized the MC3 ionizable cationic lipid from safflower edible oil, validated the formulation of the IVT-mRNA encapsulated in LNPs, and evaluated the delivery capacity of prepared mRNA-LNPs into HEK293T cells (13, 14). In the present study, we evaluated the in vitro transfection efficiency and cellular uptake of the prepared mRNA-LNPs into human immune cells and demonstrated the immunogenicity and safety of the mRNA vaccine candidate in animal models. These data support the introduction of an alternative to the cationic lipid in the mRNA-LNP formulation.

MATERIALS AND METHODS

Synthesis of IVT-mRNA and formulation of the mRNA-LNP. The DNA template for the IVT-mRNA was based on the RBD of Delta and Omicron variants (Accession No. PP084047). DNA was cloned into a pVAX1 expression vector includes backbone sequence main elements as well as the eGFP reporter gene bordered by 5' UTR, and then transcribed using the T7 ULTRA Transcription Kit (Invitrogen™) (13). To prepare the LNP solution, the aqueous phase consisting of mRNA in a sodium citrate buffer was slowly added to the ethanolic phase containing MC3 cationic lipid and other ingredients at an optimal molar ratio of 50:10:38.5:1.5. Transfection efficacy in HEK293T cells demonstrated that the LNPs enable the delivery of an adequate amount of mRNA cargo, resulting in the generation of an eGFP signal (14).

Generation of human monocyte-derived dendritic cells (mo-DCs). Whole blood samples were taken from healthy donors, and human peripheral blood mononuclear cells (PBMCs) were isolated using Ficoll's solution (Sigma-Aldrich) with a concentration gradient. The collected PBMCs were washed and then incubated with a human CD14-specific antibody (BioTechne, R & D Systems). The CD14+ monocytes were cultured at 4×10^6 cells/ml in RPMI-1640 medium (GibcoTM) supplemented with FBS (GibcoTM), antibiotic solution (GibcoTM), recombinant GM-CSF (100 ng/ml; Sigma-Aldrich), and recombinant human

IL-4 (50 ng/ml; Karmania pars gene) and incubated at 37°C for six days. The medium was replaced with a fresh one containing the same levels of GM-CSF and IL-4 every three days. The morphology of the cells was checked daily to confirm the time of DC maturation. On day 7, the cells were examined for the expression of CD11c and CD14 markers using flow cytometry (BD Biosciences).

Transfection of mo-DCs with IVT-mRNA. The 5×10^4 cells/well of mo-DCs were seeded in a 24-well plate, then incubated at 37°C, and treated with serum-free Opti-MEM I reduced serum media (GibgoTM). The mRNA-LNP and the diluted LNP solution in RPMI 1640 were directly transferred to each well. For positive control, the standard Lipofectamine MessengerMAX reagent (ThermoFisher Scientific) was used. Then the plate was incubated at 37°C for 48 h. Transfection efficiency was measured by estimating the intensity of eGFP protein expression in mRNA-LNP-transfected cells in a BD Accuri™ C6 Plus flow cytometer at excitation/emission of 488/533 nm and 488/585 nm 24 and 48 h after transfection. Flow cytometry data were then analyzed using CellQuest and FlowJo software.

Immunization of mice. This study followed the national and international laws and guidelines for the "Care and Use of Laboratory Animals" and was approved by the Razi Institute's Committee on the Ethics of Animal Experiments. Fifty female BALB/c mice, aged 6 to 8 weeks and averaging 20 grams in weight, were equally divided into five groups for the immunization experiments. The details of the grouping and immunization programs are presented in Table 1. A commercial injectable reagent was used to evaluate the efficiency of LNP as a carrier. An equal volume of IVT-mRNA was mixed with the in vivo-jetRNA® (Polyplus transfection) reagent, then the mRNA buffer was added. Positive and negative controls were considered, including the mRNA-reagent solution and PBS. The injection volume for each mouse was 100 µl, and it was administrated intramuscularly in the upper thigh. Sera were collected at one-week intervals up to 42 days post-vaccination to examine the antigen-specific antibody levels induced by the vaccine candidate. Cell-mediated immune responses were assessed by using the PBMCs collected at the end of the experiment.

Determination of humoral responses and antibody isotypes. Antibodies targeting the SARS-CoV-2 S protein were examined using an ELISA in serum samples. Briefly, each well of a 96-well ELISA microplate was coated with 2 µg/ml of recombinant S protein (ACRO Biosystems) in PBS (pH 7.2) through overnight incubation at 4°C. The plate was then blocked with blocking buffer at 37°C for 2 h after being washed twice with TPBS. The sera were diluted with blocking buffer and incubated for an additional 2 h. Subsequently, the HRP-conjugated goat anti-human IgG secondary antibody was applied at a 1:5,000 dilution. The optical density (OD) was measured at 450 nm.

To determine the antibody isotypes, the levels of antigen-specific IgG1 and IgG2a were estimated using the HRP-conjugated anti-mouse IgG1 and IgG2a antibodies, diluted at a ratio of 1:5,000.

Cytokine analysis and CD4 and CD8 expression. For quantitative measuring of intracellular cytokines and/or surface markers, PBMCs were isolated from each experimental group using Ficoll-Hypaque density gradient centrifugation. Approximately 4×10^6 of the cells in FBS-supplemented RPMI-1640 were seeded in a 96-well round-bottomed microplate. The cells were stimulated with viral S protein at a final concentration of 10 µg/ml. As a positive control, phytohemagglutinin (GibgoTM) was used at a final concentration of 5 µg/ml. Concentrations of IFN-γ and IL-4 were analyzed by ELISA kits (Mabtech AB, Sweden) in cell supernatants.

Table 1. Immunization schedule of mice vaccinated by mRNA-LNP of the SARS-CoV-2 Delta and Omicron variants

Groups	Immunization schedule
A	One dose (0.2 µg/µl) of mRNA-LNP vaccine candidate, prime at day 0
B	One dose (0.2 µg/µl) of mRNA-LNP vaccine candidate, prime at day 0 and boost at 14 days
C	LNP carrier without mRNA loading
D	IVT-mRNA chimeric construct loaded in transfection reagent
E	PBS

To evaluate the surface expression of CD4 and CD8 molecules on T lymphocyte subsets, two-color fluorochrome-labelled antibodies consisting of anti-CD8-FITC and anti-CD4-PE (BioLegend, USA) were used in flow cytometry. Cells were determined by BD FACSCalibur Flow Cytometer (BD Biosciences) and analyzed using FlowJo software.

Safety

Pyrogenicity. The presence of pyrogen or fever-inducing substrate was examined using the rabbit pyrogen test (RPT) and the cell-based mono- cyte activation test (MAT). To apply RPT, 9 healthy mature rabbits (3 for each treatment) weighing 1.8-2 Kg were maintained individually at 20-23°C. The initial body temperature was determined with a rectal thermometer (Elleb; USA) 90 min before the treatment. An amount of 1 ml/kg of rabbit weight of each mRNA-LNP, LNP, and PBS was injected through the marginal vein of the ear and the body temperature was recorded every 15 min for 3 h. According to the protocol (24), if the body temperature does not exceed 0.6°C and the total increased temperature of three rabbits in each treatment does not exceed 1.15°C, this substance is not pyrogen.

For the MAT assay, mo-DCs were grown in supplemented RPMI-1640 medium and seeded at a concentration of 2×10^5 cells/ml in a 96-well round-bottom plate. Cells were placed at 37°C, and the following day, mRNA-LNP and a diluted LNP solution in RPMI-1640 were added in quadruplicate to the plate wells. LPS solution (100 ng/ml; Sigma-Aldrich) and RPMI-1640 were included as controls, and the cells were allowed to incubate for 24 h. Supernatant from each well was collected and tested for IL-6 content using a specific ELISA kit (Pishtaz Teb, Iran).

Mouse toxicity study. The dose toxicity study was conducted on 30 female BALB/c mice. The animals were divided into three groups (n=10), and two doses of each mRNA-LNP, LNP, and PBS were injected into the quadriceps muscles of both legs on days 1 and 14. Observations on the general state of the animals' health, including feed and water consumption, local irritation, behavioral reactions, and individual body weights, were recorded for all animals. Blood and serum samples were collected at defined intervals for hematology and clinical chemistry parameter analysis. The mice were euthanized at each time point, and histological examinations were performed as part of the subchronic toxicity experiment. Tissue sections from the lungs, spleen, liver, brain, kidney, heart, lymph nodes, small intestine, and the site of injection were stained with Hematoxylin and Eosin (H&E).

Statistical analysis. The statistical analyses were conducted using the one-way ANOVA, and any differences were deemed statistically significant when the P value was less than 0.05.

RESULTS

More than 94% of the mRNA-LNP and LNP-transfected mo-DCs were alive after 24 and 48 h. Compared to control cells with 96% cell viability, no significant decrease ($P<0.05$) was found, which indicates that apoptosis did not occur after transfection of mRNA-LNP or unloaded LNP. Thus, none of the mRNA-LNP or ionizable cationic lipid MC3 synthesized from safflower oil used as the main compound for making LNP are toxic for these cells.

Transfection efficiency of mRNA-LNP formulated at a volume ratio of 20:100 mRNA: LNP was evaluated by the expression of eGFP reporter in human mo-DCs. More than 70% (72.34%) of cells expressed the eGFP reporter protein (Fig. 1). Although the fluorescence intensity of eGFP expression was estimated to be lower compared to the commercial reagent Lipofectamine (93.74%), the synthesized LNP also showed high efficiency in mRNA transfer. No significant decrease ($P<0.05$) in cells expressing eGFP was observed after two days. Thus, a small amount of mRNA can be transfected into the cell with a suitable efficiency with formulated LNP whose ionizable cat-

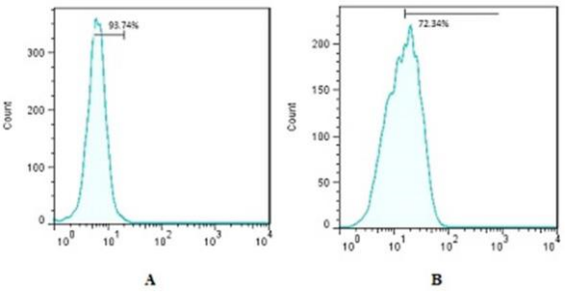

Fig. 1. Transfection efficiency of mRNA-LNP into human mo-DCs. Transfection levels as mean eGFP fluorescent signals from 1000 analyzed cells (A) transfected with mRNA-Lipofectamine and (B) transfected with mRNA-LNP complex.

ionic lipid is synthesized from safflower oil.

An ELISA was designed to assess the humoral immune responses induced by mRNA-LNP through a prime-boost vaccination scheme in mice. The results showed a significant rise (P<0.05) in the specific antibody titer against S antigen after immunization with the mRNA-LNP vaccine candidate and in the group receiving the mRNA-reagent (Fig. 2a). An increase in antibody titer in groups receiving the mRNA-LNP vaccine candidate started one week after immunization and peaked on day 21. This increase was significant (P<0.05) from day 28 (2 weeks after the booster dose) until the end of the experiment period. The decreased antibody titer in the group receiving one dose of vaccine could indicate the critical role of booster injection in the durability of the specific titer against the targeted antigen. The IgG1 isotype levels increased after the first injection of the mRNA vaccine candidate and reached the highest level after 21 days in the booster dose group. This increase was significant (P<0.05) compared to the PBS-control mice. Moreover, both vaccinated groups were positive for IgG1 or IgG2a (Fig. 2b), implying a tendency towards a Th1 immune response. The ratio was greater than 1 in mice receiving one dose, which indicates that mainly Th2-type antibody responses were induced against S antigen (Fig. 2c). After boosting, the immune responses were shifted towards the Th1 phenotype.

PBMCs collected from mice given an mRNA-LNP vaccine showed higher frequencies of S-specific IFN-γ-positive T cells compared to those that did not receive the vaccine (Fig. 3). Like the antibody findings, the strength of the cell-mediated response was influenced by the booster injection. The response level in the booster group was significantly higher (P<0.05) than in the single-dose group. Evaluation of the IL-4

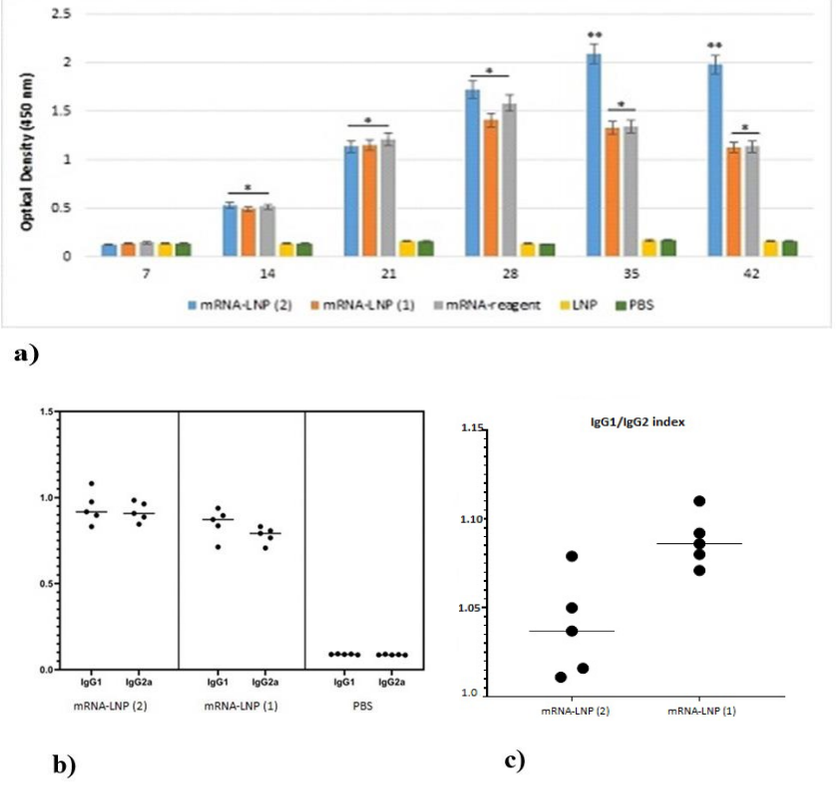

Fig. 2. a) The specific IgG antibody production against S protein in the groups of mice. * indicates a significant difference (P<0.05) in the specific antibody titer between the group receiving one dose of vaccine candidate (mRNA-LNP 1), the group receiving two doses (mRNA-LNP 2), and standard reagent mRNA with other groups. ** indicates a significant difference (P<0.05) in the specific antibody titer between the group receiving the booster dose and the other two treatment groups. b) Evaluation of IgG1 and IgG2a isotypes of specific antibodies against S protein in the groups receiving the mRNA-LNP vaccine candidate (with and without a booster dose) compared to the control group receiving PBS. c) IgG1/IgG2a ratio index isotypes before and after booster dose injection of mRNA-LNP vaccine candidate.

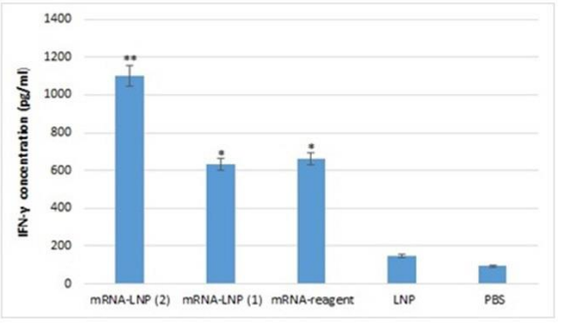

Fig. 3. Induction of IFN-γ cytokine expression in groups of mice. * indicates a significant difference (P<0.05) between the group receiving one dose of vaccine candidate (mRNA-LNP 1), the group receiving two doses (mRNA-LNP 2), and mRNA-standard reagent with other groups, ** indicates significant difference (P<0.05) between the group receiving the booster dose and the other two treatment groups.

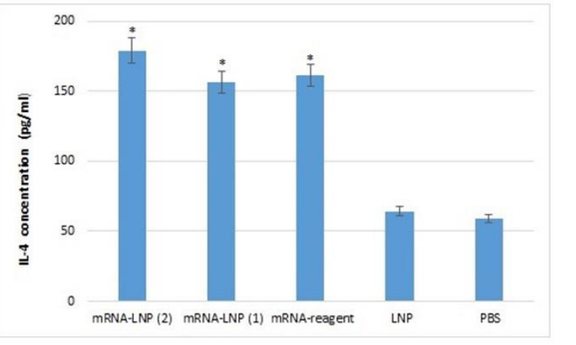

Fig. 4. Induction of IL-4 cytokine expression in groups of mice. * Indicates a significant difference (P<0.05) between the group receiving one dose of vaccine candidate (mRNA-LNP 1), the group receiving two doses (mRNA-LNP 2), and standard reagent mRNA with other groups.

levels showed an increase after the prime and boost doses in the vaccinated subjects compared to those in the control group receiving PBS (Fig. 4), which was not statistically significant (P<0.05) after boosting. The density of the dot charts increased in these groups, particularly after the booster dose was administered. The average percentages of CD4 and CD8 cells, as well as the CD4/CD8 ratio, during the 42-day immunization period are summarized in Table 2.

The body temperature of rabbits in each mRNA-LNP, LNP, and PBS injection was increased during the 3-hour monitoring in RPT. However, the changes did not exceed 0.6°C compared to the background body temperature, and its highest distribution was recorded in 38.7-38.9°C (Fig. 5).

The non-pyrogenicity of the mRNA-LNP and LNP was confirmed by quantification of the released IL-6 in MAT. LPS binding to TLR4 causes pro-inflammatory cytokines to react, especially IL-6, so it was used as a positive control. mRNA-LNP and LNP treatments did not affect the IL-6 content in human mo-DCs culture; however, cytokine secretion was significantly increased (P<0.05) in response to stimulation by LPS (Fig. 6).

After injecting mice with mRNA-LNP or LNP, a slight decrease in body temperature and weight loss was observed compared to the control mice starting 2 days post-injection. The differences were not statistically significant (P<0.05) and the injected mice quickly recovered. No inflammation or local reactions were detected after the injections in mice. Additionally, no significant biochemical or hematological changes were observed between the experimental groups compared to the control group receiving PBS, and all parameters fell within the normal range. H&E staining revealed no pathological changes in any of the examined tissues in the mRNA-LNP- or LNP-injected mice.

Table 2. Surface expression of CD4 and CD8 molecules percentages in mice vaccinated by mRNA-LNP of the SARS-CoV-2 Delta and Omicron variants

Groups	Day	CD4	CD8	CD4/CD8 ratio
A: one-dose mRNA-LNP vaccine candidate	0	6.27	4.41	1.42
	14	22.8	16.2	1.40
	21	23.5	17.8	1.32
	28	29.1	20	1.45
	42	29.8	20.3	1.46
B: two-doses mRNA-LNP vaccine candidate	21	33.5	23	1.47
	28	37.2	23.5	1.58
	42	39.1	24.7	1.58

DISCUSSION

This study described the pre-clinical development of a chimeric construct containing mRNAs encoding the Delta and Omicron RBD proteins. The mRNA-LNP vaccine candidate elicited robust immune responses following a two-dose immunization regimen in mice. Moreover, no signs of respiratory

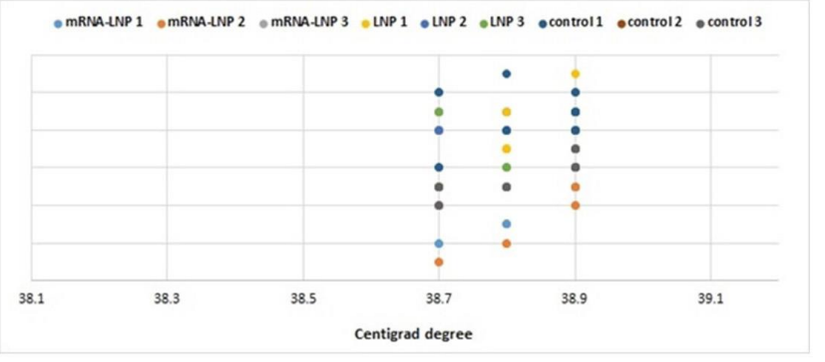

Fig. 5. Body temperature changes were tested for 3 rabbits in each of the treatments with mRNA-LNP, LNP, and PBS as a control. The highest distribution of temperature changes was recorded in the range of 38.7-38.9°C.

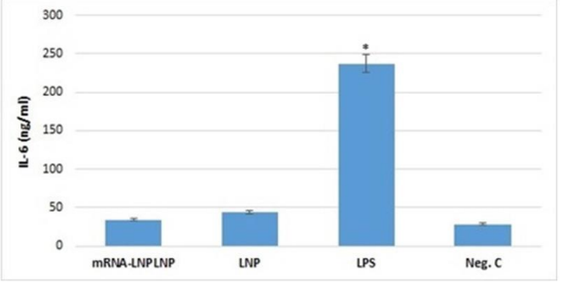

Fig. 6. Level of IL-6 secreted in human mo-DCs treated with mRNA-LNP and LNP, and stimulated with LPS in triplicate. * indicates a statistically significant difference ($P<0.05$).

distress, inflammation, or weight loss were noticed in immunized mice, highlighting the safety of the vaccine candidate. Although the approved vaccines based on the Wuhan strain S protein are effective for achieving herd immunity during the first and second waves of the COVID-19 disease (15, 16), other vaccine production approaches should be considered for adequate immunization coverage due to persistent mutations in the S gene and the emergence of numerous antigenic varieties (17, 18). The Delta variant was first detected in India on 5 October 2020 and had spread to over 179 countries by 22 November 2021. At that time, the Omicron variant carrying at least 15 substitutions in the RBD was detected. Co-circulation of the variants, which are antigenically distinct from the ancestral Wuhan-1, has overwhelmed the health system by reducing reactivity to antibodies in vaccinated individuals (19, 20). The emergence of novel recombinant circulating Omicron sub-variants, such as XBB, which has rapid global prevalence, has raised doubts about the enhanced viral infectivity, immune escape after natural infection and vaccination, and efficacy of existing vaccines (21-23).

Studies on SARS-CoV-2 vaccines have shown that the full-length S protein of the Wuhan ancestral strain is less immunogenic than newly emerged variants (24-29). The set of mutations of the S protein reduces neutralizing antibody titers against circulating variants, leading to an increase in immune escape phenomena. Hence, developing new vaccines to induce neutralizing antibodies against circulating variants is critical. It is well established that the RBD possesses the dominant neutralizing epitopes in the S protein. Monovalent or bivalent RBD-based vaccines have effectively induced neutralizing antibodies, reduced the production of non-neutralizing antibodies compared to the full-length S protein, and are effective against multiple SARS-CoV-2 variants (30-34). Therefore, we chose the RBD of the Delta and Omicron variants to improve humoral and cellular immune response. The main challenge in the transfection of mRNA is the negative charge of this molecule, which limits its crossing of the immune cell membrane passively. Therefore, different nucleic acid delivery strategies for monocytes are of interest to elicit rapid and durable protective immune responses. The positively charged cationic lipids electrostatically bind the nucleic acid in an LNP-based delivery vehicle combined with other hydrophobic moieties, enhancing mRNA delivery into DCs and activating T cells and B cells (35, 36). The high level of mRNA uptake by these antigen-presenting cells is an acceptable interpretation for the proper induction of immune responses. Previously, we detailed the synthesis of a safflower-originated ionizable lipid to formulate LNPs in the chimera RBD-mRNA delivery (14). Here, the immunogenicity of the mRNA

vaccine candidate was assessed. Mice immunized with the vaccine candidate could induce high levels of specific IgG antibodies and a robust CD8+ T cell response. The vaccine candidate elicited the subclass S-binding antibodies, which suggests a balanced Th1/Th2 immune response. Importantly, the formulated mRNA-LNP vaccine was safe, and no toxicity or significant adverse histopathological effects were seen in mouse organs.

This study demonstrated that the mRNA vaccine candidate can induce robust humoral immunity, CD8 T cell responses, and balanced Th1/Th2 antibody isotype responses following a prime/boost regimen. We suggest that the RBD chimeric construct derived from two virus variants is an effective antigen to enhance immune responses against emerging SARS-CoV-2 variants, whether used as a stand-alone vaccine or a booster shot.

REFERENCES

1. Cucinotta D, Vanelli M. WHO declares COVID-19 a pandemic. *Acta Biomed* 2020; 91: 157-160.
2. Dong Y, Dai T, Wei Y, Zhang L, Zheng M, Zhou F. A systematic review of SARS-CoV-2 vaccine candidates. *Signal Transduct Target Ther* 2020; 5: 237.
3. Krammer F. SARS-CoV-2 vaccines in development. *Nature* 2020; 586: 516-527.
4. Corbett KS, Edwards DK, Leist SR, Abiona OM, Boyoglu-Barnum S, Gillespie RA, et al. SARS-CoV-2 mRNA vaccine design enabled by prototype pathogen preparedness. *Nature* 2020; 586: 567-571.
5. Jia L, Qian SB. Therapeutic mRNA engineering from head to tail. *Acc Chem Res* 2021; 54: 4272-4282.
6. Presnyak V, Alhusaini N, Chen YH, Martin S, Morris N, Kline N, et al. Codon optimality is a major determinant of mRNA stability. *Cell* 2015; 160: 1111-1124.
7. Hanson G, Coller J. Codon optimality, bias and usage in translation and mRNA decay. *Nat Rev Mol Cell Biol* 2018; 19: 20-30.
8. Loughrey D, Dahlman JE. Non-liver mRNA delivery. *Acc Chem Res* 2022; 55: 13-23.
9. Wadhwa A, Aljabbari A, Lokras A, Foged C, Thakur A. Opportunities and challenges in the delivery of mRNA-based vaccines. *Pharmaceutics* 2020; 12: 102.
10. Lee Y, Jeong M, Park J, Jung H, Lee H. Immunogenicity of lipid nanoparticles and its impact on the efficacy of mRNA vaccines and therapeutics. *Exp Mol Med* 2023; 55: 2085-2096.
11. Shi J, Huang M-W, Lu Z-D, Du X-J, Shen S, Xu C-F, et al. Delivery of mRNA for regulating functions of immune cells. *J Control Release* 2022; 345: 494-511.
12. Tenchov R, Bird R, Curtze AE, Zhou Q. Lipid nanoparticles─ from liposomes to mRNA vaccine delivery, a landscape of research diversity and advancement. *ACS Nano* 2021; 15: 16982-17015.
13. Shahsavandi S, Hariri AA. SARS-CoV-2 Variant-Specific mRNA vaccine: Pros and cons. *Viral Immunol* 2023; 36: 186-202.
14. Shahsavandi S, Nasr Isfahani H, Hariri AA, Sharifnia Z, Soleimani S, Moradi A. Safflower-derived cationic lipid nanoparticles: potential impact on the delivery of SARS-CoV-2 mRNA transcripts. *Arch Razi Inst* 2024; 79: 1217-1226.
15. Clemente-Suárez VJ, Hormeño-Holgado A, Jiménez M, Benitez-Agudelo JC, Navarro-Jiménez E, Perez-Palencia N, et al. Dynamics of population immunity due to the herd effect in the COVID-19 pandemic. *Vaccines (Basel)* 2020; 8: 236.
16. Frederiksen LSF, Zhang Y, Foged C, Thakur A. The long road toward COVID-19 herd immunity: vaccine platform technologies and mass immunization strategies. *Front Immunol* 2020; 11: 1817.
17. Li J, Liu Q, Liu J, Fang Z, Luo L, Li S, et al. Development of bivalent mRNA vaccines against SARS-CoV-2 variants. *Vaccines (Basel)* 2022; 10: 1807.
18. Singh PK, Kulsum U, Rufai SB, Mudliar SR, Singh S. Mutations in SARS-CoV-2 leading to antigenic variations in spike protein: a challenge in vaccine development. *J Lab Physicians* 2020; 12: 154-160.
19. Antonelli M, Pujol JC, Spector TD, Ourselin S, Steves CJ. Risk of long COVID associated with delta versus omicron variants of SARS-CoV-2. *Lancet* 2022; 399: 2263-2264.
20. Kumar S, Thambiraja TS, Karuppanan K, Subramaniam G. Omicron and Delta variant of SARS-CoV-2: a comparative computational study of spike protein. *J Med Virol* 2022; 94: 1641-1649.
21. Brandolini M, Gatti G, Grumiro L, Zannoli S, Arfilli V, Cricca M, et al. Omicron sub-lineage BA. 5 and recombinant XBB evasion from antibody neutralisation in BNT162b2 vaccine recipients. *Microorganisms* 2023; 11: 191.
22. Chakraborty C, Bhattacharya M, Chopra H, Islam MA, Saikumar G, Dhama K. The SARS-CoV-2 Omicron recombinant subvariants XBB, XBB. 1, and XBB. 1.5 are expanding rapidly with unique mutations, antibody evasion, and immune escape properties–an alarming global threat of a surge in COVID-19 cases again? *Int J Surg* 2023; 109: 1041-1043.
23. Zhang QE, Lindenberger J, Parsons RJ, Thakur B, Parks R, Park CS, et al. SARS-CoV-2 Omicron XBB lineage spike structures, conformations, antigenicity, and receptor recognition. *Mol Cell* 2024; 84: 2747-2764. e7.

24. Chavda VP, Bezbaruah R, Deka K, Nongrang L, Kalita T. The Delta and Omicron variants of SARS-CoV-2: what we know so far. *Vaccines (Basel)* 2022; 10: 1926.
25. Lee IJ, Sun CP, Wu PY, Lan YH, Wang IH, Liu WC, et al. A booster dose of Delta × Omicron hybrid mRNA vaccine produced broadly neutralizing antibody against Omicron and other SARS-CoV-2 variants. *J Biomed Sci* 2022; 29: 49.
26. Li Q, Wu J, Nie J, Zhang L, Hao H, Liu S, et al. The impact of mutations in SARS-CoV-2 spike on viral infectivity and antigenicity. *Cell* 2020; 182:1284-1294. e9.
27. Pérez-Then E, Lucas C, Monteiro VS, Miric M, Brache V, Cochon L, et al. Neutralizing antibodies against the SARS-CoV-2 Delta and Omicron variants following heterologous CoronaVac plus BNT162b2 booster vaccination. *Nat Med* 2022; 28: 481-485.
28. Xu W, Wang M, Yu D, Zhang XJ. Variations in SARS-CoV-2 spike protein cell epitopes and glycosylation profiles during global transmission course of COVID-19. *Front Immunol* 2020; 11: 565278.
29. Zhang L, Cui Z, Li Q, Wang B, Yu Y, Wu J, et al. Ten emerging SARS-CoV-2 spike variants exhibit variable infectivity, animal tropism, and antibody neutralization. *Commun Biol* 2021; 4: 1196.
30. Amanat F, Thapa M, Lei T, Ahmed SMS, Adelsberg DC, Carreño JM, et al. SARS-CoV-2 mRNA vaccination induces functionally diverse antibodies to NTD, RBD, and S2. *Cell* 2021; 184: 3936-3948.e10.
31. Liu L, Wang P, Nair MS, Yu J, Rapp M, Wang Q, et al. Potent neutralizing antibodies against multiple epitopes on SARS-CoV-2 spike. *Nature* 2020; 584: 450-456.
32. Prabakaran P, Gan J, Feng Y, Zhu Z, Choudhry V, Xiao X, et al. Structure of severe acute respiratory syndrome coronavirus receptor-binding domain complexed with neutralizing antibody. *J Biol Chem* 2006; 281: 15829-15836.
33. Scheaffer SM, Lee D, Whitener B, Ying B, Wu K, Liang CY, et al. Bivalent SARS-CoV-2 mRNA vaccines increase breadth of neutralization and protect against the BA. 5 Omicron variant in mice. *Nat Med* 2023; 29: 247-257.
34. Zhang Y, Kang X, Liu S, Han P, Lei W, Xu K, et al. Broad protective RBD heterotrimer vaccines neutralize SARS-CoV-2 including Omicron sub-variants XBB/BQ. 1.1/BF. 7. *PLoS Pathog* 2023; 19(9): e1011659.
35. Eygeris Y, Gupta M, Kim J, Sahay G. Chemistry of lipid nanoparticles for RNA delivery. *Acc Chem Res* 2022; 55: 2-12.
36. Ramachandran S, Satapathy SR, Dutta T. Delivery strategies for mRNA vaccines. *Pharmaceut Med* 2022; 36: 11-20.